

Exact calculations of survival probability for diffusion on growing lines, disks, and spheres: The role of dimension

Matthew J. Simpson¹ and Ruth E. Baker²

¹*School of Mathematical Sciences, Queensland University of Technology, Brisbane, Australia*

²*Mathematical Institute, University of Oxford, Radcliffe Observatory Quarter, Woodstock Road, Oxford, United Kingdom*

(Received 28 April 2015; accepted 21 August 2015; published online 4 September 2015)

Unlike standard applications of transport theory, the transport of molecules and cells during embryonic development often takes place within growing multidimensional tissues. In this work, we consider a model of diffusion on uniformly growing lines, disks, and spheres. An exact solution of the partial differential equation governing the diffusion of a population of individuals on the growing domain is derived. Using this solution, we study the survival probability, $S(t)$. For the standard non-growing case with an absorbing boundary, we observe that $S(t)$ decays to zero in the long time limit. In contrast, when the domain grows linearly or exponentially with time, we show that $S(t)$ decays to a constant, positive value, indicating that a proportion of the diffusing substance remains on the growing domain indefinitely. Comparing $S(t)$ for diffusion on lines, disks, and spheres indicates that there are minimal differences in $S(t)$ in the limit of zero growth and minimal differences in $S(t)$ in the limit of fast growth. In contrast, for intermediate growth rates, we observe modest differences in $S(t)$ between different geometries. These differences can be quantified by evaluating the exact expressions derived and presented here. © 2015 AIP Publishing LLC. [<http://dx.doi.org/10.1063/1.4929993>]

INTRODUCTION

Mathematical models describing the transport of mass and energy by diffusion are important for improving our understanding of many applications in physics¹⁻³ and engineering.^{4,5} Unlike classical applications of reaction-diffusion theory, transport of molecules and cells in biological applications, such as during embryonic development, often involves transport processes that take place within growing tissues.⁶⁻¹⁰ In modelling these situations, individuals in the diffusing population are thought to be subject to two different transport mechanisms: (i) individuals undergo undirected diffusive motion, with diffusivity D , and (ii) individuals undergo directed motion driven by domain growth.^{11,12}

Most previous analysis of mathematical models of diffusion on a growing domain have relied on numerical solutions of the partial differential equation models governing the evolution of $C(x, t)$, the density of individuals at position x and time t .⁷⁻¹³ Recently, we have shown how to obtain exact solutions of these kinds of equations in one-dimensional Cartesian geometries.^{14,15} Analyzing these solutions and comparing them with averaged results from a discrete random walk model illustrate some fundamental differences between classical diffusion on a non-growing domain and diffusion on a growing domain. In particular, when considering a problem with a homogeneous Dirichlet (absorbing) boundary condition on a non-growing domain, it is well-known that the survival probability, $S(t)$, decays to zero as $t \rightarrow \infty$.^{1,2,16-20} In contrast, on a linearly or exponentially growing domain, we have $\mathcal{S} > 0$, where $\mathcal{S} = \lim_{t \rightarrow \infty} S(t)$, indicating there is a trade-off between the diffusive transport and domain elongation that can

leave individuals trapped on the growing domain indefinitely.¹⁵ Developing mathematical tools that can explicitly distinguish between cases where $\mathcal{S} = 0$ and $\mathcal{S} > 0$ is relevant to certain applications in developmental biology, such as the development of the enteric nervous system, where normal development is associated with conditions where a diffusing population can completely colonize a growing domain, leading to $\mathcal{S} < 1$, whereas abnormal development is associated with conditions where a diffusing population cannot completely colonize a growing domain, leading to $\mathcal{S} \equiv 1$.^{11,21-24}

In this work, we consider diffusive transport on a growing domain in one, two, and three dimensions, with rotational symmetry in the two- and three-dimensional cases. We present exact solutions to the partial differential equation models describing the diffusion of a population of individuals on a growing domain in one, two, and three dimensions. Using these solutions, we present exact expressions for the survival probability, $S_d(t)$, for $d = 1, 2$, and 3 dimensions, and we compare differences between the survival probability in different dimensions. For some parameter combinations, the $S_d(t)$ profiles are very similar regardless of the dimension, whereas for other parameter combinations, we observe differences in the $S_d(t)$ profiles, and these differences depend on the dimension of the problem. Understanding and quantifying the differences between transport phenomena in different spatial dimensions are relevant to the biophysics community since there appears to be fundamental differences in the behaviour of biological processes in two and three dimensions,^{25,26} both of which are often idealised as one-dimensional models to facilitate analysis.^{11,13,22} To corroborate our exact calculations, we also implement a stochastic random walk model

of diffusion on a growing domain in one, two, and three dimensions, and we show that numerical estimates of $S_d(t)$ from these algorithms are in good agreement with the exact calculations.

MATHEMATICAL MODEL

We consider diffusive transport on a uniformly elongating domain, $0 < x < L(t)$, and we use the same nomenclature to denote one-, two-, and three-dimensional geometries. In one dimension $L(t)$ represents the length of the tissue in the usual Cartesian coordinate system. In two and three dimensions $L(t)$ represents the radius of the growing disk or sphere, respectively. A schematic of the geometries and initial conditions relevant to our study are shown in Figure 1. We note at the outset that one of the limitations of our work is that our approach is limited to rotationally symmetric two- and three-dimensional problems and we will comment further on this restriction in the conclusions section.

Domain growth is associated with a velocity field in the elongating tissue. This velocity field causes a point within the growing tissue at location x to translate to $x + v(x,t)\tau$ during a small time interval from time t to time $t + \tau$. By considering the expansion of an element of initial width Δx , we can derive an expression relating $L(t)$ and $v(x,t)$ which can be written as

$$\frac{dL(t)}{dt} = \int_0^{L(t)} \frac{\partial v}{\partial x} dx. \quad (1)$$

For uniform growth, where $\partial v/\partial x$ is independent of position, we have $\partial v/\partial x = \sigma(t)$.^{8-10,27,28} Combining this with Equation (1) gives

$$\frac{\partial v}{\partial x} = \frac{1}{L(t)} \frac{dL(t)}{dt}. \quad (2)$$

Our assumption that the growth is uniform, so that $\partial v/\partial x$ is independent of position, is essential for our analysis. Without loss of generality, we assume that the domain elongates in the positive x -direction with $v(0,t) = 0$. Integrating Equation (2) gives

$$v(x,t) = \frac{x}{L(t)} \frac{dL(t)}{dt}. \quad (3)$$

Conservation of mass considerations for a population of diffusing individuals on a growing domain gives rise to an expression for the evolution of $C_d(x,t)$, where $d = 1, 2, 3$ refers to the dimension of the problem. The partial differential equation

governing $C_d(x,t)$ is given by

$$\frac{\partial C_d}{\partial t} = \frac{1}{x^{(d-1)}} \frac{\partial}{\partial x} \left(x^{(d-1)} D \frac{\partial C_d}{\partial x} - x^{(d-1)} v C_d \right), \quad 0 < x < L(t), \quad (4)$$

where $d = 1$ corresponds to one-dimensional Cartesian geometry, $d = 2$ corresponds to a two-dimensional disk with rotational symmetry, and $d = 3$ corresponds to a three-dimensional sphere with rotational symmetry. The first term on the right of Equation (4) is the usual second order diffusion term which represents undirected movement of individuals within the diffusing population. The second term on the right of Equation (4) is a first order advection term which represents the biased movement of individuals associated with domain growth. Previous analysis has shown that Equation (4), for $d = 1$, corresponds to the continuum limit description from a underlying random walk model on a growing domain.²⁷

To solve Equation (4), we use a boundary fixing transformation, $\xi = x/L(t)$, giving

$$\frac{\partial C_d}{\partial t} = \frac{D}{L^2(t)} \frac{1}{\xi^{(d-1)}} \frac{\partial}{\partial \xi} \left(\xi^{(d-1)} \frac{\partial C_d}{\partial \xi} \right) - \frac{dL(t)}{dt} \frac{d}{L(t)} C_d, \quad 0 < \xi < 1. \quad (5)$$

To proceed, we re-scale time,^{14,15}

$$T(t) = \int_0^t \frac{D}{L^2(s)} ds. \quad (6)$$

The relationship between $T(t)$ and $L(t)$ has important consequences. When $L(t)$ grows slower than $t^{1/2}$, such as in the non-growing case where $L(t) = L(0)$,¹⁴ we always have $T(t) \rightarrow \infty$ as $t \rightarrow \infty$. In contrast, when $L(t)$ grows faster than $t^{1/2}$, such as linear or exponential $L(t)$,¹⁴ the long time behaviour of $T(t)$ can be different and $T(t)$ may approach some positive constant as $t \rightarrow \infty$.¹⁴ This distinction is relevant to some of the results that we will present later.

Introducing the re-scaled time variable into Equation (5) gives

$$\frac{\partial C_d}{\partial T} = \frac{1}{\xi^{(d-1)}} \frac{\partial}{\partial \xi} \left(\xi^{(d-1)} \frac{\partial C_d}{\partial \xi} \right) + F_d(T) C_d, \quad 0 < \xi < 1, \quad (7)$$

where

$$F_d(T) = -\frac{d}{D} L(t) \frac{dL(t)}{dt}. \quad (8)$$

The solution of Equation (7) can be obtained by separation of variables and treating the cases $d = 1, 2$, and 3 separately.

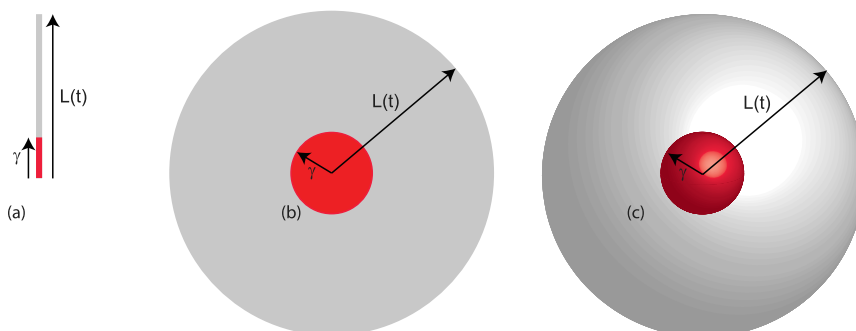


FIG. 1. Schematic diagrams showing the problem of diffusion on a growing (a) line, (b) disk, and (c) sphere. In each case, the domain is $0 \leq x \leq L(t)$ (grey), where $L(t)$ is the length of the growing line in one-dimensional Cartesian geometry whereas $L(t)$ is the radius of the growing disk and growing sphere in two and three dimensions, respectively. The initial condition corresponds to some region, $0 < x < \gamma$, with $C_d(x, 0) = 1$, as illustrated in (a)–(c) (red shading).

To make progress, we assume that we have a symmetry (zero flux) boundary condition at the origin, $\partial C_d/\partial x = 0$ at $x = 0$ (or $\partial C_d/\partial \xi = 0$ at $\xi = 0$), and an absorbing boundary condition at the moving boundary, $C_d(x, t) = 0$ at $x = L(t)$ (or $C_d(\xi, t) = 0$ at $\xi = 1$).

The solution can be written as

$$C_1(\xi, T) = \sum_{n=1}^{\infty} A_{1,n} \cos(\lambda_{1,n}\xi) \exp \left[\int_0^T F_1(T') dT' - \lambda_{1,n}^2 T \right], \quad (9)$$

$$C_2(\xi, T) = \sum_{n=1}^{\infty} A_{2,n} J_0(\lambda_{2,n}\xi) \exp \left[\int_0^T F_2(T') dT' - \lambda_{2,n}^2 T \right], \quad (10)$$

$$C_3(\xi, T) = \sum_{n=1}^{\infty} A_{3,n} \frac{\sin(\lambda_{3,n}\xi)}{\xi} \exp \left[\int_0^T F_3(T') dT' - \lambda_{3,n}^2 T \right], \quad (11)$$

where n is a positive integer, $\lambda_{1,n} = \pi(2n - 1)/2$, $\lambda_{2,n}$ are the zeros of the zeroth-order Bessel function of the first kind,²⁹ and $\lambda_{3,n} = n\pi$. In each case, the coefficients $A_{d,n}$ can be chosen so that $C_d(\xi, 0)$ matches the initial condition. For this work, inspired by Landman's previous numerical study of the development of the enteric nervous system,¹¹ we focus on the initial condition

$$C_d(x, 0) = 1 - H(x - \gamma), \quad 0 \leq x \leq L(0), \quad (12)$$

where H is the Heaviside step-function. This initial condition corresponds to some initial region of the domain, $x < \gamma$, being uniformly occupied at a maximum density, and the remaining portion of the domain being vacant, as illustrated in Figure 1 for each geometry considered. To ensure that our exact solutions match this initial condition, we specify

$$A_{1,n} = \frac{2}{\lambda_{1,n}} \sin \left(\frac{\lambda_{1,n}\gamma}{L(0)} \right), \quad (13)$$

$$A_{2,n} = \frac{2\gamma J_1(k_n\gamma)}{k_n L^2(0) J_1(k_n L(0))^2}, \quad (14)$$

$$A_{3,n} = \frac{2}{L(0)\lambda_{3,n}^2} \left[L(0) \sin \left(\frac{\lambda_{3,n}\gamma}{L(0)} \right) - \lambda_{3,n}\gamma \cos \left(\frac{\lambda_{3,n}\gamma}{L(0)} \right) \right], \quad (15)$$

where the constants k_n are chosen so that the quantity $L(0)k_n$ corresponds to the zeros of the zeroth-order Bessel function of the first kind.²⁹ With all of this information we now have exact expressions for $C_d(\xi, T)$, for $d = 1, 2$, and 3. These expressions can be re-written in terms of the physical coordinates, (x, t) , to give $C_d(x, t)$, for $d = 1, 2$, and 3, which are the relevant solutions for diffusion on a growing line, disk, and sphere, respectively.

To quantify the interplay between the diffusive motion and the domain growth we calculate the survival probability^{1,2}

$$S_d(t) = \frac{\int_0^{L(t)} C_d(x, t) dV}{\int_0^{L(0)} C_d(x, 0) dV}, \quad (16)$$

where the integration is performed with respect to the relevant volume element for each geometry: (i) for $d = 1$, we have dV

$= dx$; (ii) for $d = 2$, we have $dV = 2\pi x dx$; and (iii) for $d = 3$, we have $dV = 4\pi x^2 dx$. Evaluating these integrals gives exact expressions for the survival probability in each dimension,

$$S_1(t) = \frac{L(0)}{\gamma} \sum_{n=1}^{\infty} \frac{A_{1,n}}{\lambda_{1,n}} \sin(\lambda_{1,n}) \exp(-T\lambda_{1,n}^2), \quad (17)$$

$$S_2(t) = \frac{2L^2(0)}{\gamma^2} \sum_{n=1}^{\infty} \frac{A_{2,n}}{\lambda_{2,n}} J_1(\lambda_{2,n}) \exp(-T\lambda_{2,n}^2), \quad (18)$$

$$S_3(t) = \frac{3L^3(0)}{\gamma^3} \sum_{n=1}^{\infty} \frac{A_{3,n}}{\lambda_{3,n}^2} [\sin(\lambda_{3,n}) - \lambda_{3,n} \cos(\lambda_{3,n})] \times \exp(-T\lambda_{3,n}^2), \quad (19)$$

where the coefficients $A_{d,n}$ in Equations (17)-(19) are given by Equations (13)-(15), respectively. We will now evaluate these expressions and make comparisons between the results in different geometries. The results are presented here for general $L(t)$. In this work, we will make use of linear and exponential $L(t)$, for which some useful properties are summarized in Table I.

Since our exact expressions for $S_d(t)$ are infinite series, we anticipate that it is possible to develop useful approximations to the long time behaviour of $S_d(t)$ by adopting a leading eigenvalue approximation of Equations (17)-(19). This amounts to retaining only the first term in the infinite series,

$$S_d(t) \sim A_{1,d} \exp \left(-\lambda_{1,d}^2 T(t) - \frac{d}{D} \int_0^{T(t)} L(T') \frac{dL(T')}{dT'} dT' \right). \quad (20)$$

This approximation shows that the decay of $S_d(t)$ is controlled by the time dependence of $T(t)$. If $T(t) \rightarrow \infty$ as $t \rightarrow \infty$, as in the case of a non-growing domain,¹⁴ then $S_d(t)$ will eventually decay to zero regardless of d . Alternatively, if $T(t)$ approaches a finite value as $t \rightarrow \infty$, such as when we have exponential or linear $L(t)$ (Table I), then $S_d(t)$ may approach a non-zero limit as $t \rightarrow \infty$. The leading eigenvalue expression for $S_d(t)$ is of interest because it explicitly shows the trade-off between effects of domain growth and the diffusion of individuals on the domain. We will explore the accuracy of such an approximation in the Results and Discussion section.

RESULTS AND DISCUSSION

Since an unbiased random walk on a d -dimensional hypercubic lattice with unit spatial and temporal steps is associated with a diffusivity $D = 1/(2d)$, we will set $D = 1/2$, $D = 1/4$, and $D = 1/6$ in one, two, and three dimensions, respectively.³ As well as presenting a comparison of exact expressions for $S_d(t)$ in different dimensions, we also use a discrete random

TABLE I. Mathematical relationships for exponential and linear domain growth functions.

$L(t)$	$T(t)$	$t(T)$	$F_d(T)$
$L(0)\exp(\alpha t)$	$\frac{D(1-\exp(-2\alpha t))}{2\alpha L^2(0)}$	$\frac{1}{2\alpha} \log_e \left(\frac{D}{D-2\alpha L^2(0)T} \right)$	$\frac{dL^2(0)\alpha}{2\alpha L^2(0)T-D}$
$L(0) + \beta t$	$\frac{D t}{L(0)(L(0) + \beta t)}$	$\frac{L^2(0)T}{D-L(0)\beta T}$	$\frac{d\beta L(0)}{L(0)T\beta-D}$

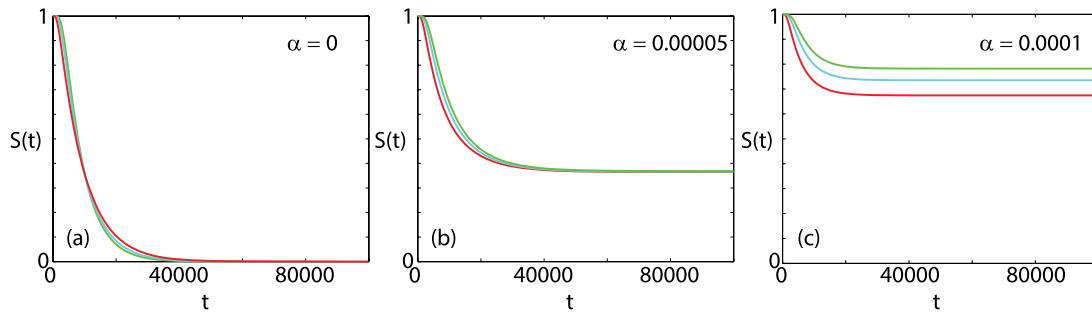


FIG. 2. Comparison of the survival probability, $S_d(t)$, for diffusion on an exponentially growing line (red), disk (cyan), and sphere (green) for the (a) non-growing domains, $\alpha = 0$, (b) moderate domain growth, $\alpha = 0.00005$, and (c) more rapid domain growth, $\alpha = 0.0001$. All results are shown for $0 < t < 100\,000$ with $L(0) = 100$, $\gamma = 20$ and $D = 1/2, 1/4$, and $1/6$ for diffusion on a line, disk, and sphere, respectively. All results are calculated by truncating the infinite series for $S(t)$ after 100 terms, and we checked that this level of truncation is sufficient to ensure that the results are insensitive to this choice.

walk analogue of our mathematical model to provide a numerical estimate of $S_d(t)$. A description of this discrete model and a comparison between the numerical estimates of $S_d(t)$ and the exact results in one, two, and three dimensions are given in the supplementary material.³⁰

Results in Figure 2(a) show the survival probabilities for the standard cases of diffusion on a non-growing line, disk, and sphere. These results confirm that $S \equiv 0$ in each geometry. Furthermore, comparing the $S_d(t)$ profiles between different geometries indicates that not only is the long time survival probability identically zero for each geometry but we also observe a very similar transient decay from $S_d(0) = 1$ in each geometry. Results in Figure 2(b) illustrate $S_d(t)$ on a line, disk, and sphere that undergoes significant exponential growth during the time interval shown. Comparing these profiles with the non-growing results in Figure 2(a) illustrates that one of the key novelties for diffusive processes on growing domains is that the long time survival probability can be positive in the case of a growing domain, indicating that a certain proportion of the initial population remains on the growing domain indefinitely. In this case, we have $S_d \approx 0.37$, indicating that approximately 37% of the initial population never reaches the absorbing boundary at $x = L(t)$ and, as a result, approximately 37% of the initial population remains on the growing domain indefinitely. Comparing results in Figures 2(a) and 2(b), we see that the transient and long term $S_d(t)$ profiles are very different when comparing the non-growing and growing domain problems; however, when we compare $S_d(t)$ profiles for different geometries under the same growth conditions we observe very similar transient and very similar long time behaviour.

Results in Figure 2(c) compare $S_d(t)$ profiles on a growing line, disk, and sphere for a faster growth rate than in Figure 2(b). Comparing the three different $S_d(t)$ profiles in Figure 2(c) indicates that we observe a modest difference in the survival probability, both in the long time steady-state behaviour and the short time transient behaviour. For this case in one-dimensional Cartesian geometry, we have $S_1 \approx 0.67$, for two-dimensional cylindrical geometry, we have $S_2 \approx 0.74$, and for three-dimensional spherical geometry, we have $S_3 \approx 0.78$, indicating that the survival probability differs by approximately 11% between the different geometries. Comparing results in Figures 2(b) and 2(c), it is at first tempting to imagine that further increasing the rate of domain growth could lead to further differences in the properties of $S_d(t)$

between different geometries. However, further increasing the rate of domain growth, keeping everything else constant, leads to a situation where $S_d(t) \equiv 1$ for all t as the transport process becomes completely dominated by domain growth, regardless of the dimension of the problem, and all of the initial profile remains on the rapidly growing domain indefinitely. Therefore, it is difficult to draw very general conclusions about the role of dimension in the survival probability for diffusion processes on growing lines, disks, and spheres since, for certain problems, we observe practically identical short time transient results and practically identical long time results. In contrast, for other combinations of parameters, the trade-off between diffusion and growth can lead to differences in both the short time and long time survival probabilities. In summary, in the limits of zero growth and rapid growth, the differences in $S_d(t)$, between different geometries, are very small. However, for intermediate growth rates that are most biologically relevant, we observe that $S_d(t)$ can be different depending on the geometry of the problem. These differences can be explored, and quantified, by evaluating the exact solutions presented here.

In addition to evaluating the exact expressions for $S_d(t)$ to produce the results in Figure 2, we may also estimate the long time survival probability by implementing a leading eigenvalue approximation, given by Equation (20). To demonstrate the effectiveness of this approximation, we re-compute the long time survival probability for the problems reported previously in Figure 2(c). The exact calculation for the one-dimensional problem gives $S_1(100\,000) = 0.674$ whereas the leading eigenvalue approximation gives $S_1(100\,000) = 0.676$, correct to three decimal places. Therefore, for this problem, the error introduced by retaining just one term in the infinite series is very small, approximately 0.3%, and we also find that apply the leading eigenvalue approximation to the two- and three-dimensional calculations in Figure 2(c) leads to reasonably accurate estimates of the long time survival probability. In addition to computing the long time survival probability using a leading eigenvalue approximation, it is also possible to S_d using a limit definition, given by

$$S_d = \lim_{t \rightarrow \infty} \frac{1}{t} \int_0^t S_d(t') dt'. \quad (21)$$

However, since the leading eigenvalue approximation, given Equation (20), turns out to be very simple to implement, we do not implement Equation (21) here.

CONCLUSION

The transport of molecules and cells in many applications during embryonic development is complicated by the fact that the substrate through which the transport takes place grows simultaneously. In this work, we present exact mathematical expressions that govern the survival probability for diffusive transport on growing lines, disks, and spheres. These expressions are a significant generalization of classical models describing the survival probability on non-growing domains where the long time survival probability, S_d , asymptotes to zero as $t \rightarrow \infty$. Instead, on a growing domain, we can have $S_d > 0$ provided that $L(t)$ grows faster than $t^{1/2}$, indicating that a certain proportion of the diffusing population remains trapped on the domain in the long time limit. Alternatively if $L(t)$ grows slower than $t^{1/2}$, then S_d asymptotes to zero as $t \rightarrow \infty$. This result is analogous to previous analyses of the survival probability in expanding cages, receding cliffs,^{1,2} and parabolic geometries.^{31,32} In these previous studies, the motion of individuals within the diffusing population is not driven by the underlying expansion of the domain, whereas in the biologically inspired problems we consider, the motion of individuals in the population is coupled to the growth of the domain through the advection term in Equation (4).

Using our exact solutions, we compare $S_d(t)$ for problems on growing lines, disks, and spheres and show that, in both the limit of zero growth and the limit of very fast growth, the survival probability is very similar regardless of dimension. In contrast, for intermediate growth rates, we observe differences in $S_d(t)$ depending on the dimension of the problem. In particular, these differences occur both in the early time $S_d(t)$ behaviour as well as the long time limit where $S_d(t)$ can asymptote to a positive constant, S_d . Although all of our results and analysis are presented for one particular biologically inspired choice of initial condition, $C_d(x, 0)$, our solution strategy can be adapted for other choices of $C_d(x, 0)$. Using appropriate orthogonality results, we can choose the coefficients, $A_{d,n}$, to match other choices of initial condition. Another application of the present work is that our exact solutions for $S_d(t)$ enable the calculation of the probability density function of the exit time distribution, $\phi_d(t) = -dS_d(t)/dt$, which means that all the moments of the exit time distribution can be obtained from our exact expressions for $S_d(t)$,^{1,19,20} thereby providing further information about the trade-off between diffusion and growth on growing lines, disks, and spheres.

There are several options for extending the analysis presented here. One of the restrictions of our present work is that we consider rotationally symmetric two- and three-dimensional problems since we can re-cast the governing partial differential equation for $C_d(x, t)$ in terms of one spatial variable. A different approach would be required if we were to analyse $S_d(t)$ for asymmetric two- and three-dimensional problems since the exact solution technique described here does not apply. Instead, we could solve for the density function, and hence $S_d(t)$, using a numerical approach. Another

extension would be to consider the case where the growth is not spatially uniform and $\partial v/\partial x$ depends upon position. This kind of nonuniform growth problem leads to additional advection terms in the partial differential equation for $C_d(x, t)$,¹³ and we anticipate that analytical progress might be possible for certain choices of $\partial v/\partial x$ only.

ACKNOWLEDGMENTS

We appreciate support from the Australian Research Council (Grant No. FT130100148), and we sincerely thank two anonymous referees who provided very helpful suggestions.

- ¹S. Redner, *A Guide to First Passage Processes* (Cambridge University Press, 2001).
- ²P. L. Krapivsky, S. Redner, and E. Ben-Naim, *A Kinetic View of Statistical Physics* (Cambridge University Press, 2010).
- ³B. D. Hughes, *Random Walks in Random Environments* (Oxford University Press, 1995).
- ⁴J. Bear, *Dynamics of Fluids in Porous Media* (Elsevier, 1971).
- ⁵R. B. Bird, W. R. Stewart, and E. N. Lightfoot, *Transport Phenomena* (John Wiley and Sons, 2002).
- ⁶L. Wolpert, *Principles of Development* (Oxford University Press, 2011).
- ⁷S. Kondo and R. Asai, *Nature* **376**, 765 (1995).
- ⁸K. J. Painter, P. K. Maini, and H. G. Othmer, *Proc. Natl. Acad. Sci. U. S. A.* **96**, 5549 (1999).
- ⁹E. J. Crampin, E. A. Gaffney, and P. K. Maini, *Bull. Math. Biol.* **61**, 1093 (1999).
- ¹⁰E. J. Crampin, W. W. Hackborn, and P. K. Maini, *Bull. Math. Biol.* **64**, 747 (2002).
- ¹¹K. A. Landman, G. J. Pettet, and D. F. Newgreen, *Bull. Math. Biol.* **65**, 235 (2003).
- ¹²B. J. Binder, K. A. Landman, M. J. Simpson, M. Mariani, and D. F. Newgreen, *Phys. Rev. E* **78**, 031912 (2008).
- ¹³M. J. Simpson, K. A. Landman, and D. F. Newgreen, *J. Comput. Appl. Math.* **192**, 282 (2006).
- ¹⁴M. J. Simpson, *PLoS One* **10**, e0117949 (2015).
- ¹⁵M. J. Simpson, J. A. Sharp, and R. E. Baker, *Phys. Rev. E* **91**, 042701 (2015).
- ¹⁶J. Franke and S. N. Majumdar, *J. Stat. Mech.: Theory Exp.* **2012**, P05024.
- ¹⁷M. Chupeau, O. Benichou, and S. N. Majumdar, *Phys. Rev. E* **91**, 032106 (2015).
- ¹⁸A. J. Bray and S. N. Majumdar, *J. Phys. A: Math. Gen.* **39**, L625 (2006).
- ¹⁹A. Ryabov and P. Chvosta, *J. Chem. Phys.* **136**, 064114 (2012).
- ²⁰A. Ryabov, *J. Chem. Phys.* **138**, 154104 (2013).
- ²¹D. F. Newgreen, B. Southwell, L. Hartley, and I. J. Allan, *Acta Anat.* **157**, 105 (1996).
- ²²K. A. Landman, M. J. Simpson, and D. F. Newgreen, *Dev., Growth Differ.* **49**, 277 (2007).
- ²³R. McLennan, L. Dyson, K. W. Prather, J. A. Morrison, R. E. Baker, P. K. Maini, and P. M. Kulesa, *Development* **139**, 2935 (2012).
- ²⁴H. M. Young, A. J. Bergner, M. J. Simpson, S. J. McKeown, M. M. Hao, C. R. Anderson, and H. Enomoto, *BMC Biol.* **12**, 23 (2014).
- ²⁵P. Friedl, E. Sahai, S. Weiss, and K. M. Yamada, *Nat. Rev. Mol. Cell Biol.* **13**, 743 (2012).
- ²⁶K. Konstantopoulos, P.-H. Wu, and D. Wirtz, *Biophys. J.* **104**, 279 (2013).
- ²⁷R. E. Baker, C. A. Yates, and R. Erban, *Bull. Math. Biol.* **72**, 719 (2009).
- ²⁸C. A. Yates, R. E. Baker, R. Erban, and P. K. Maini, *Phys. Rev. E* **86**, 021921 (2012).
- ²⁹M. Abramowitz and I. A. Stegun, *Handbook of Mathematical Functions with Formulas, Graphs, and Mathematical Tables* (Dover, 1965).
- ³⁰See supplementary material at <http://dx.doi.org/10.1063/1.4929993> for results from the discrete algorithm.
- ³¹I. Peschel, L. Turban, and F. Iglói, *J. Phys. A: Math. Gen.* **24**, L1229 (1991).
- ³²L. Turban, *J. Phys. A: Math. Gen.* **25**, L127 (1992).